

# Quadruplet codon decoding-based versatile genetic biocontainment system

Yun-Nam Choi<sup>1,†</sup>, Donghyeon Kim<sup>1,†</sup>, Seongbeom Lee<sup>1</sup>, Ye Rim Shin<sup>1</sup> and Jeong Wook Lee<sup>1,2,\*</sup>

<sup>1</sup>Department of Chemical Engineering, Pohang University of Science and Technology (POSTECH), Pohang 37673, Republic of Korea

<sup>2</sup>School of Interdisciplinary Bioscience and Bioengineering (I-Bio), Pohang University of Science and Technology (POSTECH), Pohang 37673, Republic of Korea

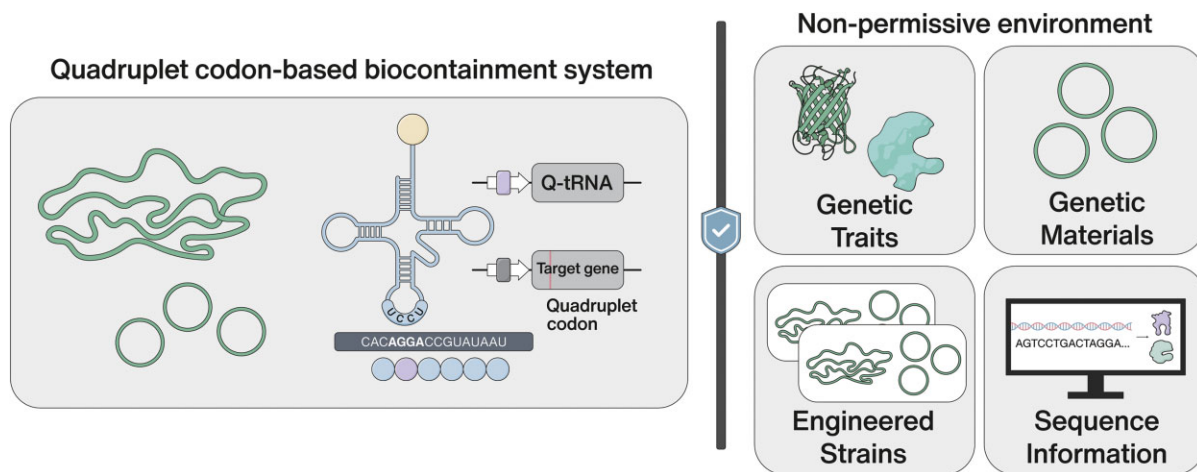
\*To whom correspondence should be addressed. Tel: +82 54 279 2337; Fax: +82 54 279 5528; Email: jeongwook@postech.ac.kr

†The first two authors should be regarded as Joint First Authors.

## Abstract

Biological resources, such as sequence information, genetic traits, materials and strains, pose risks when inadvertently released or deliberately misused. To address these concerns, we developed Quadruplet COdon DEcoding (QCODE), a versatile genetic biocontainment strategy that introduces a quadruplet codon (Q-codon) causing frameshifts, hindering proper gene expression. Strategically incorporating Q-codons in multiple genes prevents genetic trait escape, unallowed proliferation of microbial strains and unauthorized leakages of genetic materials. This multifaceted strategy, integrating Q-codons for genetic traits, materials and strains, ensures robust biocontainment across various levels. Notably, our system maintains sequence protection, safeguarding genetic sequence information against unauthorized access. The QCODE approach offers a versatile, efficient and compact solution to enhance biosecurity in diverse biological research settings.

## Graphical abstract



## Introduction

Recent advancements in biotechnology have facilitated the exploration and manipulation of genes and strains derived from nature, resulting in the emergence of novel biological resources. These resources possess substantial potential for advancing life-saving therapeutics and promoting the sustainable production of biofuels and chemicals. However, there exists an evident risk of the inadvertent release of these resources into non-permissive environments in various forms, including genes, strains and sequence information (1–5). Such releases may occur either accidentally or intentionally. Once bi-

ological resources breach non-permissive environments, they can potentially rapidly proliferate, replicate and pose harm to the surrounding environment. Moreover, the theft or unauthorized acquisition of strains, genomes, genes or sequences, whether physical material or digital data, presents a significant security concern. In the event of theft, malicious entities can easily synthesize, clone and functionally restore sequence data. Several biocontainment systems have been proposed in response to the imperative need to safeguard against unauthorized proliferation, misuse and espionage of biological resources (6–9).

Received: May 23, 2024. Revised: November 22, 2024. Editorial Decision: December 15, 2024. Accepted: December 20, 2024

© The Author(s) 2025. Published by Oxford University Press on behalf of Nucleic Acids Research.

This is an Open Access article distributed under the terms of the Creative Commons Attribution-NonCommercial License

(<https://creativecommons.org/licenses/by-nc/4.0/>), which permits non-commercial re-use, distribution, and reproduction in any medium, provided the original work is properly cited. For commercial re-use, please contact [reprints@oup.com](mailto:reprints@oup.com) for reprints and translation rights for reprints. All other permissions can be obtained through our RightsLink service via the Permissions link on the article page on our site—for further information please contact [journals.permissions@oup.com](mailto:journals.permissions@oup.com).

The conventional auxotrophic biocontainment system disrupts genes responsible for the biosynthesis of essential substances, including nucleic acids or amino acids (10–13). However, this approach can be circumvented when cells acquire nutrients that are deficient in their surroundings. To address this challenge, synthetic auxotrophy, involving the use of non-canonical amino acids or DNA/RNA analogs that are inaccessible to the natural environment (14,15), has emerged and proven effective in reducing the escape frequency. Alternatively, genetic circuits controlling the expression of essential genes or toxins have been devised (16–22), wherein the activation of crucial genes or repression of toxins depends on the presence of specific small molecules.

Although these approaches have made significant progress in achieving genetic biocontainment at the organism level, they still have limitations in preventing the transfer of genetic materials to other organisms through horizontal gene transfer, potentially leading to the inadvertent proliferation of genetically modified organisms (GMOs) (23,24).

Clustered regularly interspaced short palindromic repeats (CRISPR) technology, a programmed DNA degradation tool, has been utilized to eliminate recombinant DNA from cells at defined time points (25). Sense codon reassignment is another strategy to impede horizontal gene transfer between different organisms. By introducing novel genetic codes that surpass the interpretation capabilities of native organisms, this approach can effectively prevent proper decoding and functional expression of genetic material when transferred to other organisms (26–29). These strategies can prevent the transfer of genetic materials to other organisms but often require extensive genome manipulation. Developing a simpler and more universally applicable method would facilitate the broader implementation of biocontainment systems.

In this study, we present a versatile, efficient and compact genetic biocontainment system centered around quadruplet codon (Q-codon) decoding to confine all types of biological resources, such as genetic traits, genetic material, strains and sequence information, exclusively to a permissive environment by adopting Q-codons instead of the universal triplet codon.

## Materials and methods

### Biological resources

**Strains and cultivation.** *Escherichia coli* DH10 $\beta$  was used for cloning and plasmid construction. *E. coli* DH10 $\beta$  and *E. coli* MG1655 were used for protein expression and Q-codon tests. MG1655 was the parental strain used for genome engineering, which included *argW* and essential gene knockouts and mutations of AGGA to AGAA in 14 essential genes (Supplementary Table S1).

For cell cultivation, Luria–Bertani (LB) medium was used in liquid or solid form, and appropriate antibiotics were added as needed (kanamycin, 50  $\mu$ g/ml; carbenicillin, 100  $\mu$ g/ml; gentamicin, 30  $\mu$ g/ml; and chloramphenicol, up to 34  $\mu$ g/ml; all purchased from GoldBio). Unless stated otherwise, cells were grown at 37°C overnight, and agitation at 200 rpm was conducted for the liquid cultures. Cells carrying a temperature-sensitive plasmid were grown at 30°C (Supplementary Table S2). Cell growth was monitored by measuring the optical density at 600 nm (OD<sub>600</sub>) using a spectrophotometer (Biochrom Biodrop Duo, Thermo Fisher Scien-

tific, Waltham, MA, USA) or a multi-plate reader (Hidex Sense 425-301, Turku, Finland).

### Plasmid and strain construction

Unless stated otherwise, all polymerase chain reaction (PCR) experiments were conducted using Q5 polymerase [New England Biolabs (NEB), Boston, MA, USA] according to the manufacturer's protocol. Moreover, the PCR products were treated with DpnI (NEB) and purified (PCR purification kit, GeneAll Biotechnology, Seoul, Republic of Korea) when necessary. All oligonucleotides used in this study (Supplementary Table S3) were purchased from Cosmo Genetech (Seoul, Republic of Korea). Short DNA fragments were prepared using oligo-dimerization ( $\leq$  90 bp) or polymerase cycling assembly (PCA; 90 bp < DNA  $\leq$  200 bp). Oligo-dimerization was conducted using the following procedures: (i) mixing two oligonucleotide fragments with complementary sequences; (ii) heating them at 95°C for 2 min; and (iii) slowly cooling them to room temperature for 1 h. For PCA, two seed oligonucleotides (up to 90 nt), in which the sequences were complementary at their 3' ends in the 20-nt length, were hybridized, and each end was extended using PCR (~15 cycles). Primers targeting each end were added to the reaction mixture for regular PCR amplification.

Plasmids were constructed using TA cloning (Promega), restriction enzyme digestion and ligation, or Gibson assembly (NEB). All constructs were confirmed using colony PCR (AccuPower PCR premix, Bioneer, Oakland, CA, USA) and sequence analysis (Cosmo Genetech). Mutations, including single nucleotide replacements or insertions into plasmids, were performed using a site-directed mutagenesis kit (NEB) or self-Gibson assembly. For both methods, the plasmid was linearized by PCR using a primer set designed to include the desired mutation at the appropriate position (Supplementary Table S3). For self-Gibson assembly, one primer was designed to include at least a 20 nt overhang that was complementary to the other primer to form overlapping ends using PCR. The details regarding plasmid construction are provided in Supplementary Table S2.

Plasmids were transformed using heat shock or electroporation, and the resulting strains were confirmed using colony PCR and sequence analysis. We knocked out *argW* from the *E. coli* MG1655 genome using lambda ( $\lambda$ ) red recombineering, as described previously (30,31), and confirmed its knockout using PCR and sequence analysis.

### Cos- and CRISPR-optimized MAGE recombineering: Cos-CRMAGE

For genome editing, we combined co-selection multiplex automated genome engineering (Cos-MAGE) with CRISPR-optimized MAGE (CRMAGE) (32–34). Two plasmids, pMA7CR\_2.0 and pMAZ-SK, were gifts from Alex Nielsen (plasmids # 73 950 and # 73 962, Addgene, Watertown, MA, USA) (32). The gene encoding the tetracycline repressor, *tetR*, was inserted into pMA7CR\_2.0, yielding pMA7CR\_2.0\_tetR. The *E. coli* MG1655  $\Delta$ *argW* strain containing pMA7CR\_2.0\_tetR was used as a starter culture, and each single guide RNA (sgRNA) gene for negative selection was cloned into pMAZ-SK, resulting in 14 different plasmids (Supplementary Table S2). An overnight starter culture was inoculated into fresh LB medium containing carbenicillin and grown to an OD<sub>600</sub> of 0.5. The  $\lambda$  red recombinase expression

was induced using 0.2% L-arabinose for 15 min, and the cells were immediately chilled on ice for another 15 min. The pelleting and re-suspension steps were repeated twice to make the cells electrocompetent. Then, the cells were re-suspended in sterilized cold water containing MAGE oligonucleotides (total concentration up to 10  $\mu$ M) and one of the sgRNA-expressing plasmids (~250 ng), followed by electroporation. The cells were recovered for an hour in 1 ml of LB medium supplemented with carbenicillin in a 15 ml culture tube. The cells were further grown for 2 h with kanamycin and another 2 h with 200 ng/ml anhydrotetracycline (ATc). The cells were collected, washed twice with fresh LB medium and inoculated into 4 ml of LB medium containing carbenicillin, ATc and 0.2% L-rhamnose for overnight culture. The entire process was repeated using the overnight culture as a starter for the next cycle. In the final cycle, cells were spread onto LB agar plates containing carbenicillin, ATc and L-rhamnose to obtain a single colony.

AGGA to AGAA mutations in the genome were confirmed using multiplex allele-specific colony PCR (MASC-PCR) (33,34). Two primer sets were designed to target the wild-type (WT) and mutant gene loci for each mutation target. The reverse primers were identical, but the forward primers differed in their last nucleotides at the 3' end (G/A). For *mrdB*, *ycfQ* and *foldC*, the reverse primers differed in their last nucleotide at the 3' end (C/T), whereas the forward primers were identical (Supplementary Table S3). Amplicon loci were designed to produce PCR bands of different lengths in a single PCR (Supplementary Table S4). The optimum annealing temperature ( $T_m$ ) was determined experimentally using a WT colony as a template. At the end of the Cos-CRMAGE cycle, MASC-PCR was performed to identify the mutant strain with the maximum number of mutations in its genome (AccuPower PCR premix, Bioneer). Colonies identified as potential mutant strains with MASC-PCR were confirmed using sequence analysis (Cosmo Genetech).

The insertion of the Q-codon into essential genes was similarly performed using CRMAGE with four modifications: (i) the MG1655 WT  $\Delta argW$  strain was transformed with pMA7CR\_tetR\_QtRNAw (Supplementary Table S2) to guarantee a constitutive expression of Q-tRNAw during mutation; (ii) a single round of CRMAGE was conducted with only one MAGE oligonucleotide; (iii) an additional silent mutation to remove the PAM site around the Q-codon site was included in the MAGE oligonucleotide (Supplementary Table S3) for negative selection; and (iv) after confirming the mutations, the plasmid pMA7CR\_tetR\_Q-tRNAw was replaced with another plasmid, pH.Tet-QtRNAw, which carried an ATc-inducible expression cassette for the Q-tRNAw (Supplementary Table S2). Two essential genes, *fldA* and *cysS*, were mutated, resulting in Q-*fldA* and Q-*cysS* strains, respectively (Supplementary Table S2).

### Protein production analysis

For green fluorescent protein (GFP) production analysis, an overnight culture was inoculated into fresh LB medium containing appropriate antibiotics at an initial  $OD_{600}$  of 0.05. Gene expression was induced by 1 mM isopropyl- $\beta$ -D-1-thiogalactopyranoside (IPTG) when the  $OD_{600}$  reached 0.4. This was followed by a 6 h cultivation. GFP fluorescence ( $\lambda_{ex}$ , 485 nm;  $\lambda_{em}$ , 535 nm) was measured using a microplate reader (Hidex Sense 425-301) and normalized to the cell den-

sity ( $OD_{600}$ ). The cells were collected and lysed using sonication. His-tagged proteins were purified using an Ni-NTA column (Ni-NTA Spin Kit, #31 314, Qiagen, Hilden, Germany) and analyzed using sodium dodecyl sulfate-polyacrylamide gel electrophoresis (SDS-PAGE) on a 4–12% gel (NuPAGE Bis-Tris, #NP0326BOX, Invitrogen, Waltham, MA, USA). The GFP bands were excised, digested with trypsin (Promega, Madison, WI, USA) and subjected to matrix-assisted desorption ionization-time of flight (MALDI-TOF) analysis (Autoflex Speed LRF, Bruker Daltonics, Billerica, MA, USA). The peak list was generated using Flex Analysis 3.4. For the peak-picking threshold, 500 for minimum resolution of monoisotopic mass, 5.0 for S/N. Analyses were performed by Genomine, Gyeongsangbuk-do, Republic of Korea.

Antimicrobial peptide (AMP) production was analyzed with minor modifications. Gene expression was induced using 1 mM IPTG and 0.2% L-arabinose, followed by overnight incubation at 30°C. For protein identification, protein spots were excised after SDS-PAGE, digested with trypsin (Pierce™ Trypsin Protease, MS Grade, 90 058; Thermo Fisher Scientific) and subjected to MALDI-TOF analysis (ABSciex TripleTOF 5600+, SCIEX, Framingham, MA, USA). Analyst® TF 1.7.1 (operation), ProteinPilot™ 4.5 (sequence analysis) and PeakView 2.20 (chromatogram/manual analysis) were used for analysis. Analyses were outsourced to Life Science Laboratories Co., Seoul, Republic of Korea.

### tREX analysis

For tRNA extension (tREX) analysis, a native tRNA<sup>Arg</sup><sub>CCU</sub> knockout strain ( $\Delta argW$ ) was used. An overnight culture was diluted with 50 ml of 2× YT medium containing appropriate antibiotics and grown at 37°C. When the  $OD_{600}$  reached 0.5–1, the cells were collected by centrifugation, and the pellet was washed twice with 800  $\mu$ l and 450  $\mu$ l of buffer D [150 mM NaCl, 50 mM sodium acetate (pH 5), 10 mM MgCl<sub>2</sub> and 0.1 mM EDTA], being centrifuged for 2 min at 7400 rpm between the wash steps. For cell lysis, 50  $\mu$ l of liquefied phenol was added to the cells, followed by head-over-tail rotation for 15 min at 15 rpm. The supernatant from centrifugation at 14 500 rpm for 25 min at 4°C was mixed with 500  $\mu$ l of chloroform by vigorous vortexing for 1 min. Subsequent centrifugation at 14 500 rpm for 1 min resulted in two-layer separation, and the top layer containing tRNAs (~480  $\mu$ l) was transferred to a new tube.

The tRNA extracts were processed in three different ways based on a previous method (35) with some modifications. (i) A 136  $\mu$ l tRNA extract was mixed with 40  $\mu$ l of buffer D and precipitated with ethanol by incubation for 1 h at 4°C, followed by the removal of supernatants after centrifugation at 14 500 rpm for 25 min and drying. The precipitated sample was re-suspended with buffer D to a final concentration of 1  $\mu$ g/ $\mu$ l (Biochrom Biodrop Duo, Thermo Fisher Scientific), resulting in positive control for full extension. (ii) A 136  $\mu$ l tRNA extract was mixed with 8  $\mu$ l of 600 mM NaOH and incubated for 1 h at 42°C. Next, 16  $\mu$ l of 3 M sodium acetate (pH 5.2) and 100 mM NaIO<sub>4</sub> were added, followed by 1.5 h of further incubation. Ethanol precipitation was conducted as previously described, resulting in a negative control for no extension. (iii) A 136  $\mu$ l tRNA extract was mixed with 24  $\mu$ l of buffer D and 16  $\mu$ l of 100 mM NaIO<sub>4</sub>. After 1.5 h of incubation at room temperature, the sample was precipitated with ethanol as previously described, resulting in a testing sample.

To confirm probe specificity, the tRNA extract from the untransformed  $\Delta argW$  strain was processed in the same way as the testing sample.

For extension, 2  $\mu$ l of the processed tRNAs were mixed with 5  $\mu$ l of NEBuffer 2.1, 1  $\mu$ l of dNTPs (10 mM each), 1  $\mu$ l of Cy5-labeled DNA probe (1  $\mu$ M, Bioneer) and 40.5  $\mu$ l of nuclease-free water. The annealing reactions were conducted in a thermocycler (Applied Biosystems, Foster City, CA, USA) with the following settings: 95°C for 1 min, 70°C for 2 min and 50°C for 2 min. This was followed by incubation at 4°C. Then, 0.5  $\mu$ l of the exo(-) Klenow fragment with no 3'→5' exonuclease activity (M0212S, NEB) was added, and this was followed by incubation for 20 min at 37°C. To confirm the extension, each reaction was mixed with 2× loading dye (8 M urea and 0.04% Orange G) and run on an 8% PAGE gel [acrylamide (19:1)] at 200 V for 45 min. After staining with SYBR Gold Nucleic Acid Gel Stain (Invitrogen), the gel was imaged using Azure 600® (700 nm).

### Lycopene measurement

An overnight culture was inoculated into fresh LB medium containing appropriate antibiotics at an initial OD<sub>600</sub> of 0.05. Gene expression was induced using 1 mM IPTG and 0.2% L-arabinose when the OD<sub>600</sub> reached 0.4. The cells were grown for 12 h at 30°C. Lycopene was extracted by adding acetone to cell pellets and heating them for 15 min at 55°C (36). The lycopene content was compared by measuring the absorbance at 470 nm and normalizing it using cell density (Hidex Sense 425-301).

### Survival assays

#### Kanamycin resistance

Overnight cultures grown in LB medium supplemented with carbenicillin were washed twice and diluted (1:10 000). Approximately 5  $\mu$ l of the cultures were loaded on the LB agar plate supplemented with kanamycin (50  $\mu$ g/ml) and grown overnight at 37°C.

#### Plasmid replication initiation

Two plasmids, pQtrfA-oriV and pH.BAD-Q-tRNA<sub>w</sub>, were co-transformed with the MG1655 WT  $\Delta argW$  strain. After 1 h of recovery, the cells were spread onto two separate plates: one containing kanamycin and arabinose (0.2%) and the other containing kanamycin only. After 16 h, colonies on the plates were imaged using Azure 600®. A single colony from a plate containing kanamycin and arabinose was inoculated into LB medium supplemented with kanamycin and 0.2% L-arabinose. The overnight culture was washed twice and inoculated into 2 ml of fresh LB medium. After incubation for 12 h, the cells were diluted to 1:20 000 with fresh LB medium containing kanamycin. Exactly 100  $\mu$ l of the diluted culture was transferred onto a 96-well microplate (CLS3904, Corning, Corning, NY, USA) and grown with or without arabinose induction. Cell growth was monitored by measuring the cell density (OD<sub>600</sub>) every 2 h for 16 h (Hidex Sense 425-301).

For quantitative PCR analysis, an overnight culture of each strain was inoculated into LB medium supplemented with carbenicillin (OD<sub>600</sub>: 0.05) and grown for 16 h, both with and without Q-tRNA expression. Plasmid extraction was then performed using the Exprep plasmid SV kit (GeneAll Biotechnology, Seoul, Republic of Korea). Amplification was con-

ducted according to the manufacturer's protocol (TOPreal SYBR Green qPCR Premix, Enzynomics and Applied Biosystems 7500 Fast Real-Time PCR Instrument system, Thermo Fisher Scientific). The reaction mixture contained 3 ng of template DNA, 10  $\mu$ l of 2× master mix, 1  $\mu$ l each of 10  $\mu$ M primer (Supplementary Table S3) and nuclease-free water to a final volume of 20  $\mu$ l. For the negative control, nuclease-free water was used instead of template DNA.

### Essential gene

Single colonies of the Q-fldA and Q-cysS strains were grown overnight. An overnight culture of each strain was washed twice and diluted (1:20 000) with fresh LB medium containing carbenicillin. With or without ATc, cell growth was monitored by measuring the cell density (OD<sub>600</sub>) every 2 h for 16 h (Hidex Sense 425-301). The overnight culture was serially diluted in phosphate-buffered saline (PBS) over a 6-log range, and 5  $\mu$ l of each dilution was spotted onto LB agar plates containing carbenicillin and ATc. The plates were imaged using Azure600® (True Color Imaging, Azure Biosystems, Dublin, CA, USA).

An overnight culture of each strain was inoculated into LB medium supplemented with carbenicillin and ATc (OD<sub>600</sub>: 0.05) and grown until it reached an OD<sub>600</sub> of 1. The cells were collected by centrifugation, washed twice with fresh LB medium and plated onto two separate plates (both supplemented with carbenicillin), one with ATc and one without. The number of colonies on each plate was counted after 1, 3 and 8 days to calculate the escape frequency.

## Results

### Arginine incorporation by the native translation system of *E. coli* at the quadruplet codon

We sought to restrict genetic traits, genetic material, strains and sequence information to a permissive environment where the corresponding canonical amino acid can accurately be assigned to the Q-codon by an *E. coli* native translation system. This process required the identification of a compatible pair of *E. coli* native translation system-derived tRNA and aminoacyl-tRNA synthetases. As Q-codons invariably include one of the existing triplet codons, avoiding unintended cross-reactions was imperative. Therefore, we focused on rare codons in *E. coli*, specifically targeting the two rarest codons encoding arginine, AGG and AGA (Supplementary Table S5). Initially, we replaced the anticodons of the two cognate tRNAs, tRNA<sup>Arg</sup><sub>CCU</sub> and tRNA<sup>Arg</sup><sub>UCU</sub>, with UCCU, resulting in the creation of Q-tRNA<sub>w</sub> and Q-tRNA<sub>u</sub>, respectively. We substituted the original triplet codon, 31R, in GFP with the Q-codon, AGGA, and introduced a silent mutation at the 45L site, changing it from CTG to CTT. This alteration caused premature translation termination in the case of incorrect Q-Codon DEcoding (QCODE; Figure 1A; Supplementary Table S1).

We confirmed successful Q-GFP expression using both Q-tRNAs employing fluorescence (Figure 1B) and SDS-PAGE (Figure 1C). Conversely, the negative control strains lacking Q-tRNAs did not exhibit fluorescence or full-length translation (Figure 1B, C). Arginine incorporation at the Q-codon site was validated using MALDI-TOF analysis (Figure 1D). Additionally, we verified the *in vivo* aminoacylation status of Q-tRNA<sub>w</sub> using the tREX method (35). Briefly, the tREX

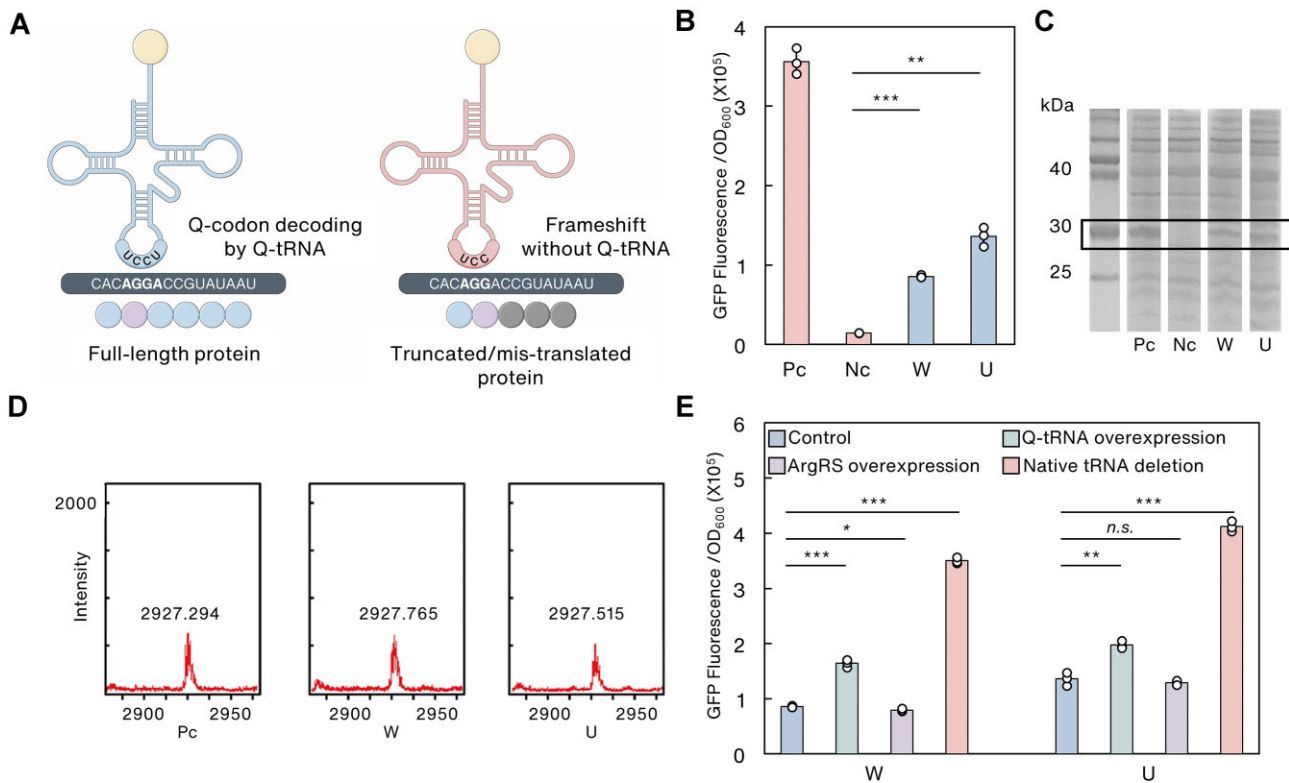


**Figure 1.** Incorporation of arginine into the protein via a quadruplet codon (AGGA). **(A)** Translation of the protein with and without the engineered Q-tRNA capable of reading the quadruplet codon (AGGA). Correct decoding of the AGGA codon as arginine by the Q-tRNA produces a full-length protein, whereas incorrect decoding results in premature translation termination or mistranslation. **(B–D)** Confirmation of full-length and functional protein translation using GFP fluorescence **(B)**, SDS-PAGE **(C)** and MALDI-TOF analysis **(D)**. We replaced the original triplet codon in GFP at the 31R site with AGGA and expressed it with and without the Q-tRNAs. Our analysis in **(B)** and **(C)** demonstrates the production of a full-length GFP in the strains containing the Q-tRNAs (W and U). Conversely, the negative control strain (Nc) lacking the Q-tRNA did not exhibit fluorescence or full-length translation. MALDI-TOF analysis **(D)** demonstrates the arginine incorporation at the Q-codon sites. **(E)** Overexpression of Q-tRNAs or ArgRS, or deletion of native tRNA ( $tRNA^{Arg_{CCU}}$ ), enhancing QCODE. To reduce the probability of the first three nucleotides (AGG) of the Q-codon being occupied by the native tRNAs, we expanded the pool of arginine-charged Q-tRNAs by increasing the expression of Q-tRNAs or ArgRS or by deleting one of the native tRNAs for arginine. Reducing the competition between Q-tRNAs and native tRNAs resulted in a substantial increase in QCODE efficiency. Pc, GFP with a silent mutation at 45L (positive control); Nc, GFP with mutations at 31R and 45L (Q-GFP; negative control); Wm, Q-GFP and Q-tRNAw; U, Q-GFP and Q-tRNAu. All graphs represent the mean  $\pm$  SD, with  $n = 3$ . Unpaired  $t$ -tests were used for comparisons in **(B)** and **(E)**. \* $P < 0.05$ , \*\* $P < 0.01$ , \*\*\* $P < 0.001$ ; n.s., not significant.

method helps detect specific tRNAs using a fluorescently labeled DNA probe (Supplementary Figure S1). Moreover, this technique helps determine the charging status of the tRNA by observing its elongation. Specifically, the 3' end of non-charged tRNAs undergoes oxidation, which prevents elongation, leading to a shorter band (Supplementary Figure S1). Conversely, charged (aminoacylated) tRNAs are protected from oxidation, facilitating their elongation and resulting in a longer band (Supplementary Figure S1). We exclusively detected Q-tRNAw among the total tRNAs extracted from cells expressing Q-tRNAw (Supplementary Figure S2; lanes 2–4 compared with lane 1). Notably, Q-tRNAw produced an extended band (Supplementary Figure S2; lane 4), confirming its aminoacylation.

### Engineering strategies to improve QCODE

Although the Q-tRNAs were correctly charged with arginine and capable of decoding the Q-codon, the expression of Q-GFP was noticeably lower than that of the WT GFP, lacking the Q-codon (Figure 1B). To enhance the QCODE efficiency, we speculated that the first three nucleotides (AGG) of the Q-codon (AGGA) could still be occupied by the native

tRNAs, *argW* and *argU*, rather than the Q-tRNAs. Therefore, we hypothesized that increasing the pool of arginine-charged Q-tRNAs or reducing the presence of competitive native tRNAs would improve QCODE using Q-tRNAs. To expand the pool of arginine-charged Q-tRNAs, we explored two approaches: increasing the expression of Q-tRNA or ArgRS (Supplementary Table S2). We observed that increasing the Q-tRNA expression facilitated enhanced Q-GFP expression, whereas elevating ArgRS expression did not have a comparable effect (Figure 1E).

Subsequently, to mitigate the competition between native tRNAs and Q-tRNAs, we knocked out one of the native tRNAs for arginine.  $tRNA^{Arg_{CCU}}$  (*argW*) exclusively incorporates arginine into the AGG codon; however, the AGG codon can also be decoded by another tRNA,  $tRNA^{Arg_{UCU}}$  (*argU*). Thus, the deletion of  $tRNA^{Arg_{CCU}}$  was expected to have a lesser impact on cellular fitness. Notably,  $\Delta argW$  strains exhibited a substantial increase in QCODE efficiency with both Q-tRNAs (Figure 1E), revealing that competition between Q-tRNA and native tRNA had limited efficient QCODE. The expression of the Q-tRNAs in the  $\Delta argW$  strain enabled Q-GFP to undergo full-length translation comparable with the WT strain (Figure 1B, E).

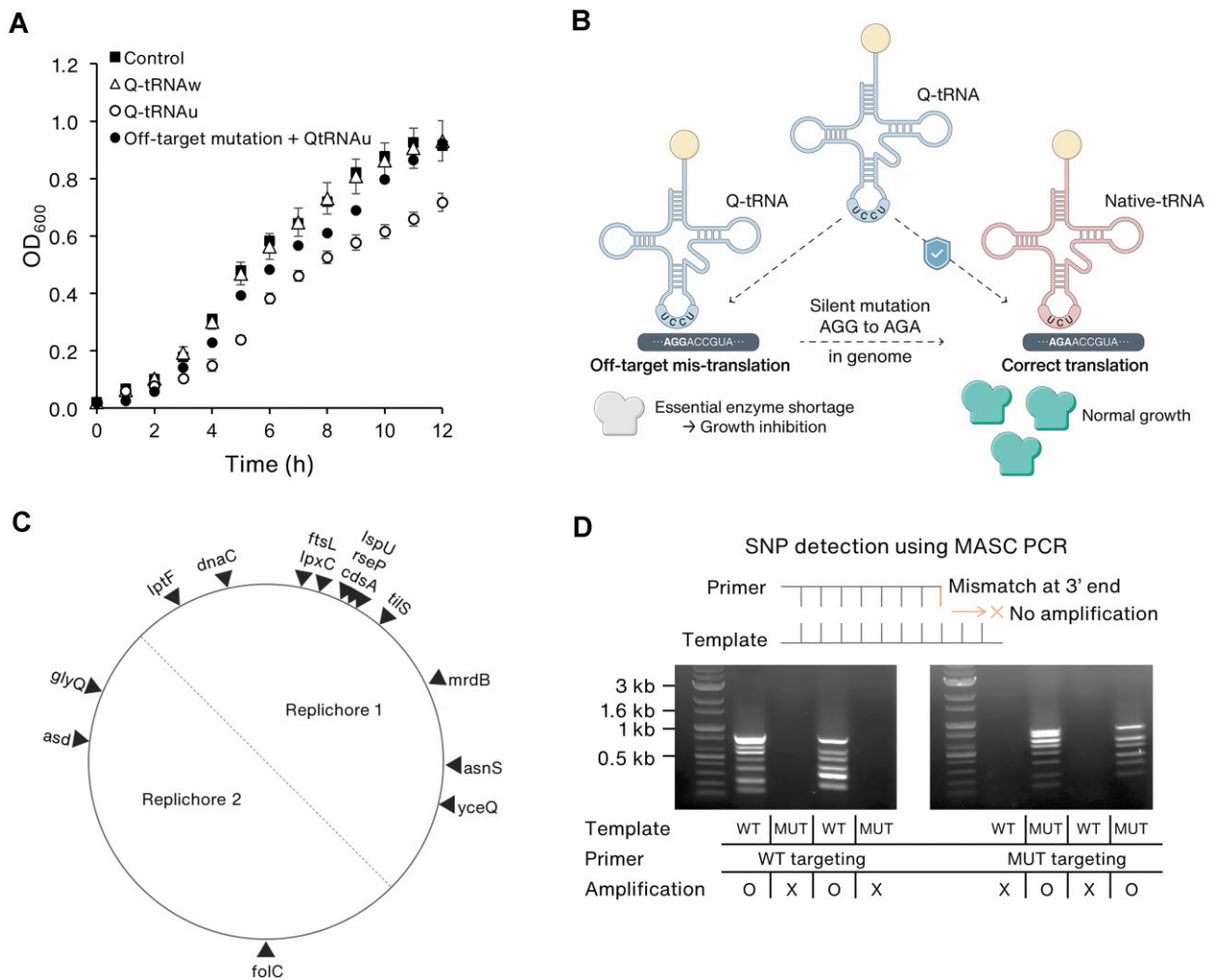


**Figure 2.** Utilizing genome engineering to minimize off-target decoding using Q-tRNA<sub>u</sub>. Q-tRNA<sub>u</sub> expression in the  $\Delta argW$  strain markedly reduced cell growth, unlike Q-tRNA<sub>w</sub> (A). This suggests that Q-tRNA<sub>u</sub>'s higher QCODE efficiency may introduce unintended frameshifts in essential genes (B). To minimize the off-target effect, the arginine codon was changed from AGG to AGA in 14 essential genes (C) through Cos-CRMAGE (see Supplementary Figure S3). The 14 desired mutations in the genome were confirmed via MASC-PCR (D) as described in detail elsewhere (33,34). The method employs three primers per mutation target: two primers distinguish between wild-type (WT) and mutant (MUT) sequences at their 3' terminus, while sharing a common third primer (top). Each colony from Cos-CRMAGE is tested with separate PCRs using either WT- or MUT-specific primer sets. Successful amplification occurs only with MUT primers when the colony carries the desired mutation. We designed primers to produce unique band sizes for all 14 mutation targets (Supplementary Table S4), enabling efficient screening. The gel images below show results from pooled PCR samples. Lanes 1–4, PCR run with WT targeting primers; 5–8, PCR run with MUT targeting primers; 1, 3, 5, 7, PCR run with WT colony; 2, 4, 6, 8, PCR run with MUT colony; 1, 2, 5, 6, PCR run with primers targeting *lpxC*, *cdsA*, *glyQ*, *asd*, *folC*, *asnS*, *yceQ* and *lptF*; 3, 4, 7, 8, PCR run with primers targeting *mrdb*, *ispU*, *rseP*, *tlpS*, *dnaC* and *ftsL*. Cell growth recovery (A) was achieved by changing the arginine codon from AGG to AGA in 14 essential genes ( $n = 3$ , error bars indicate  $\pm$  SD).

### Genome engineering to minimize off-target decoding by Q-tRNA<sub>u</sub>

In contrast to Q-tRNA<sub>w</sub>, Q-tRNA<sub>u</sub> expression in the  $\Delta argW$  strain impeded cell growth (Figure 2A). We hypothesized that the higher efficiency of Q-tRNA<sub>u</sub> (Figure 1B) might cause unintended frameshifts in non-target genes, potentially leading to the mistranslation of essential genes. We intended to use the case of Q-tRNA<sub>u</sub> to exemplify the mechanisms to reduce or mitigate off-target effects when employing Q-codon-based genetic biocontainment systems. Specifically, when essential genes incorporate the AGG codon for arginine and have an 'A' immediately following it, the four-base sequence AGGA might be erroneously recognized as the Q-codon by the Q-tRNAs (Figure 2B). Napolitano *et al.* revealed that 123 arginine codons in the essential genes of *E. coli* were represented

as AGG/AGA (37). We identified that 14 contained AGGA sequences within their coding sequences (CDSs) (Figure 2C; Supplementary Table S1). Thus, we sought to replace these 14 AGGAs in the genome with AGAAs, preventing potential off-target decoding by Q-tRNAs while preserving their original amino acid sequences.

To efficiently edit the genome, we combined Cos-MAGE (33) and CRMAGE (32), resulting in Cos-CRMAGE (Supplementary Figure S3). Using this approach, we successfully generated a mutant strain, MUT  $\Delta argW$ , in which the 14 desired AGAA mutations were seamlessly incorporated into the genome (Figure 2D). Subsequently, we introduced Q-tRNA<sub>u</sub> into the MUT  $\Delta argW$  strain. We observed that cell growth recovered (Figure 2A), confirming that minimizing potential off-target decoding by Q-tRNAs can benefit

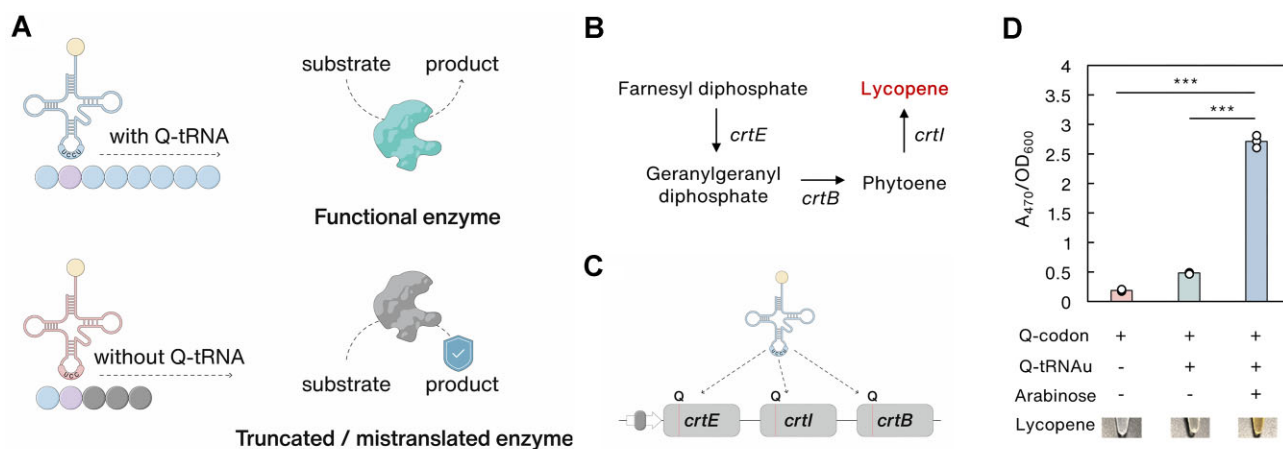


**Figure 3.** QCODE biocontainment system for genetic trait protection. **(A)** Q-codon incorporation into a gene for a specific genetic trait and regulation of its expression by QCODE will confine the genetic trait in a permissive environment. **(B)** Lycopene biosynthesis pathway. **(C)** Introduction of Q-codons into three enzymes for lycopene production with Q-tRNAu co-expression under the arabinose-inducible promoter. **(D)** Lycopene production was observed in the presence of Q-tRNAs. The graph represents the mean  $\pm$  SD ( $n = 3$ ). Unpaired  $t$ -tests were used for comparisons. \* $P < 0.05$ , \*\* $P < 0.01$ , \*\*\* $P < 0.001$ .

cell growth. Consequently, we used Q-tRNAu for the mutant  $\Delta argW$  strain (MUT  $\Delta argW$ ) and Q-tRNAw for the WT  $\Delta argW$  strain (WT  $\Delta argW$ ).

### QCODE as a means for genetic biocontainment

Following the proficient decoding of the Q-codon using a native translation system-derived approach, we validated the QCODE system as a genetic biocontainment mechanism to safeguard genetic traits and material, engineered strains and sequence information.

#### QCODE to prevent leakage of genetic traits

We hypothesized that Q-codon incorporation into a target gene would effectively restrict unintended gene expression and genetic traits in a non-permissive environment lacking the QCODE system (Figure 3A). To test our hypothesis, we used the QCODE system with Q-tRNAw in the WT  $\Delta argW$  strain to control antibiotic resistance gene expression, specifically inserting the Q-codon into the kanamycin resistance gene. This ensured that only cells with Q-tRNAw survived kanamycin exposure (Supplementary Figure S4).

Subsequently, we applied the QCODE system to control heterologous metabolic pathways. The lycopene production pathway, comprising geranylgeranyl diphosphate synthase (CrtE), phytoene synthase (CrtB) and phytoene desaturase (CrtI; Figure 3B), was selected as the target metabolic pathway. We introduced the Q-codon into all three enzymes and evaluated lycopene production in correlation with Q-tRNAu expression in the MUT  $\Delta argW$  strain (Figure 3C). As we placed the Q-tRNAu gene under the control of the arabinose-inducible promoter,  $P_{BAD}$ , to govern Q-tRNA expression, lycopene was exclusively produced only in the presence of arabinose (Figure 3D). Collectively, these results demonstrate the ability of the QCODE system to regulate gene expression, highlighting its utility in confining genetic traits within a permissive environment.

#### QCODE to prevent genetic material leakage

Genetic materials, such as plasmids, can be disseminated into the environment or transferred to other microorganisms via

horizontal gene transfer, posing potential environmental or health risks. We developed a preventive measure against genetic material leakage into non-permissive environments by leveraging the QCODE system.

TrfA is a replication initiation factor and binds to the *oriV* region to initiate plasmid replication (27,38). Accordingly, we postulated that plasmids exclusively harboring *oriV* as their replication origin and featuring TrfA with the Q-codon within its CDS would be unable to persist in a non-permissive environment lacking the QCODE system (Figure 4A). To validate this hypothesis, we created a plasmid containing the *trfA* gene containing a Q-codon (Q-trfA), along with *oriV* and *kanR*. Kanamycin resistance served as our indicator for plasmid maintenance. We transformed the plasmid into the WT  $\Delta argW$  strain carrying a Q-tRNAw-expressing plasmid under the arabinose-inducible promoter. On kanamycin-supplemented media, colonies appeared exclusively in the Q-tRNAw expression condition, indicating that the plasmid-bearing *oriV* could not be maintained within the assay limits in cells when the QCODE system was inactive (Supplementary Figure S5). Similarly, in liquid culture, cell growth was only observed in the presence of Q-tRNAw (Figure 4B; Supplementary Table S2).

Using quantitative PCR (qPCR), we measured plasmid DNA levels in cultures grown with and without Q-tRNA expression. The cycle threshold ( $C_t$ ) values from non-permissive conditions matched those of a water-only negative control (Supplementary Figure S6). Calculations of relative DNA content based on these  $C_t$  values revealed a  $> 10^5$ -fold reduction under non-permissive conditions (Figure 4C). These results demonstrate that the QCODE system can effectively restrict genetic material proliferation by making DNA replication dependent on permissive conditions.

#### QCODE to prevent engineered strain leakage

We hypothesized that introducing the Q-codon into an essential enzyme responsible for cell growth would increase its dependency on QCODE, impeding unintended proliferation in a non-permissive environment (Figure 5A). Accordingly, we selected two enzymes, flavodoxin A and cysteine-tRNA ligase

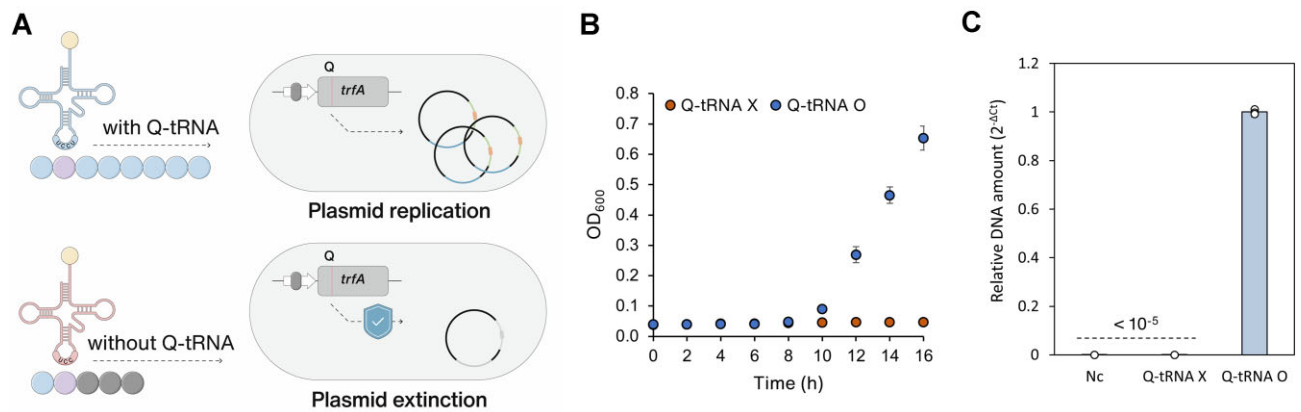


**Figure 4.** QCODE biocontainment system for genetic material protection. **(A)** Incorporation of the Q-codon into the replication initiator protein (TrfA) ensures plasmid maintenance only in cells with an active QCODE system, protecting genetic material. **(B)** Cells transformed with a plasmid carrying the Q-codon-inserted TrfA and kanamycin resistance were grown with and without Q-tRNAw expression in kanamycin-supplemented media. Cell growth was exclusively observed in the presence of Q-tRNA, indicating that the plasmid can only be maintained in cells when the QCODE system is active. **(C)** Plasmids were extracted from both cultures and quantified using quantitative PCR (qPCR). Based on the Ct value from the qPCR, the relative amount of DNA remaining in the strains was calculated ( $2^{-\Delta C_t}$ ). The higher amount of DNA in cells with the active QCODE system showed that the proliferation of genetic materials can be restricted in a non-permissive environment by rendering its replication dependent on the QCODE system. For the negative control, nuclease-free water was used instead of plasmid DNA. All graphs represent the mean  $\pm$  SD, with  $n = 3$ .

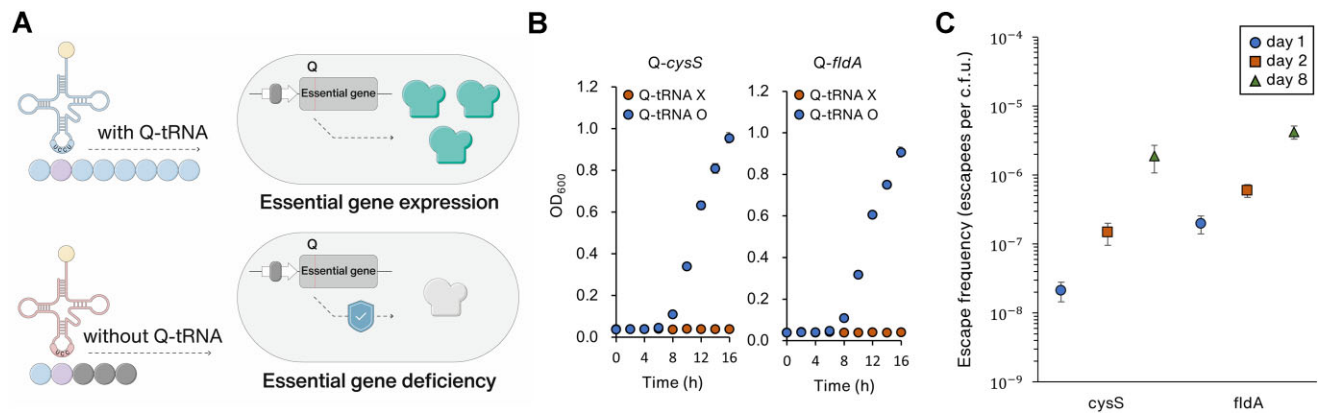


**Figure 5.** QCODE biocontainment system for engineered strain protection. **(A)** Introduction of Q-codons into essential enzymes regulates cell growth via the QCODE system, ensuring engineered strain protection. **(B)** Strains carrying the Q-codon in the essential genes showed cell growth exclusively in the active QCODE condition. **(C)** Cells were grown in a non-permissive condition for 1, 3 and 8 days, followed by colony counting. Escape frequencies increased gradually over time. All graphs represent the mean  $\pm$  SD, with  $n = 3$ .

(Supplementary Table S1), which are essential for cell growth (39).

We created two mutant strains by replacing one of the arginine codons in *fldA* or *cysS* with AGGA, rendering their decoding solely dependent on Q-tRNA expression. We observed that cells survived only when the Q-tRNAs were expressed via ATc induction, representing a permissive environment (Figure 5B; Supplementary Figure S8), suggesting the effective prevention of the proliferation of engineered strains in a non-permissive environment in the absence of survival signals.

We next investigated the robustness of our system over a longer time frame. Two strains containing the Q-codon in *cysS* or *fldA*, respectively, were grown in a permissive environment for 1 day and then moved to a non-permissive environment to see if there were escapees. The escape frequencies of the Q-cysS and Q-fldA strains on the first day were close to  $10^{-8}$  and  $10^{-7}$ , respectively, and the escape frequency gradually increased over time (Figure 5C), comparable with escape frequency reported previously in a single essential

or lethal gene (14,40,41). Extended pre-cultures in a permissive environment similarly showed increased escape frequencies after 3 days (Supplementary Figure S7). Notably, the sequencing analysis on the escapees showed that no colonies carried mutations that reverse the quadruplet codon to a triplet codon in the essential genes or disrupt the regulation of Q-tRNA expression (i.e. no mutations on the expression cassettes of Q-tRNA or repressors) (Supplementary Table S3). This may suggest that accumulated leaky expression of the Q-tRNA contributes to the occurrence of escapees over time.

### Versatility and efficacy of the QCODE system

The simplicity and adaptability of the QCODE system render it an ideal solution applicable to diverse scenarios of containment. We aimed to demonstrate the flexibility of QCODE, especially when integrating multiple layers of protection (Figure 6A). Eight distinct strains, each featuring 0–3 Q-codons,



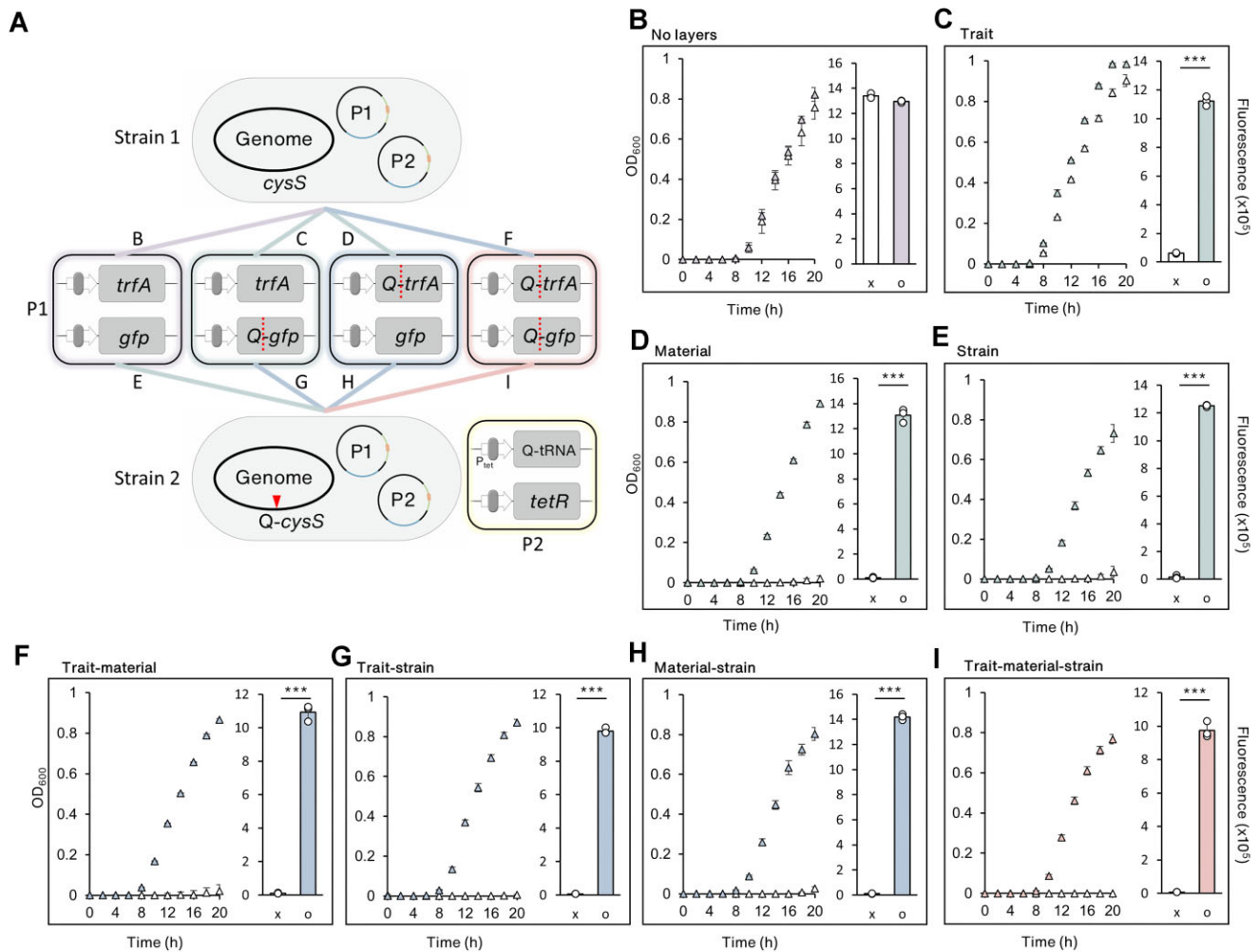


**Figure 6.** QCODE system as a preventive measure against the leakage of biological resources at multiple levels. **(A)** A genetic biocontainment approach based on the QCODE system prevents leakage of biological resources, including genetic traits (*gfp*), genetic materials (*trfA*) and engineered strains (*cysS*), at multiple levels. *cysS* is located in the genome; the others are located in plasmid 1 (P1). These genes can be designed with or without Q-codons. Plasmid 2 (P2), present in all variants, carries the Q-tRNA expression cassette and repressor. We constructed eight system variants by combining two strains with four different P1 plasmids. **(B–I)** Survival assays (left) and GFP fluorescence measurements (right) demonstrate the prevention of genetic traits, genetic material and engineered strain leakage individually and simultaneously. In scatter plots (left), colored triangles represent strains under permissive conditions (+ATc; with Q-tRNA expression), while white triangles show non-permissive conditions (–ATc; without Q-tRNA expression). In bar graphs (right), O and X denote permissive (+ATc; with Q-tRNA expression) and non-permissive conditions (–ATc; without Q-tRNA expression), respectively. All graphs represent the mean  $\pm$  SD, with  $n = 3$ . Unpaired *t*-tests were used for comparisons, \*\*\* $P < 0.001$ .

were systematically designed to secure genetic traits (*gfp*), genetic materials (*trfA*) and cell growth (*cysS*). These were arranged in a combinatorial manner to create different levels of containment, ranging from no layers to triple-layered systems [configurations: no layers (Figure 6B), trait (Figure 6C), material (Figure 6D), strain (Figure 6E), trait–material (Figure 6F), trait–strain (Figure 6G), material–strain (Figure 6H) and genetic trait–material–strain (Figure 6I)]. Each strain was equipped with a plasmid for Q-tRNA expression that was inducible under ATc conditions.

The biocontainment effectiveness of each strain was evaluated by culturing them in permissive (+ATc) and non-permissive (–ATc) environments. Monitoring cell growth and GFP fluorescence under these conditions (displayed on the left and right sides of each panel in Figure 6B–I) revealed that the inability to produce full-length GFP without QCODE confined GFP fluorescence or genetic traits to permissive (+ATc) environments. Genetic material protection was achieved by

inhibiting plasmid replication in non-permissive environments owing to the absence of functional TrfA, leading to the loss of antibiotic resistance and cell death. Strain protection was evident through the absence of essential gene (*cysS*) expression, resulting in cell death under non-permissive conditions.

Collectively, our findings suggest that when combined, these protection mechanisms effectively confined the designated bioresources as programmed, highlighting the flexibility and multilayered protection of the QCODE system.

Throughout our experiments, cell growth and fluorescence were observed exclusively in the presence of the QCODE system (Figure 6C–I). These findings highlight the effectiveness of the QCODE system in robustly safeguarding biological resources, including genetic traits, materials and strains, at various levels. The adaptability of QCODE to a range of scenarios highlights its potential as a universal tool for genetic biocontainment.

## QCODE for sequence encryption

While safeguarding genetic material and strains is conventional, protecting sequence information from unauthorized access or theft is equally crucial. Our QCODE-based genetic biocontainment system can help conceal protein sequences and their identities. Introducing the Q-codon to decode a target protein alters the nucleotide sequence of the corresponding gene, causing a frameshift when decoded in the absence of a QCODE system. This frameshift extends to sequence analysis, where the nucleotide sequence downstream of the Q-codon is misread as an erroneous amino acid sequence, leading to premature termination. Concurrently, we intentionally incorporated the Q-codon into the target sequence. We hypothesized that unauthorized users analyzing nucleotide sequences containing the Q-codon would interpret them as incorrect amino acid sequences, thereby concealing the true protein sequence and identity.

We selected three relatively short AMPs with arginine near their N-terminus for proof of concept. A comparative analysis of amino acid and nucleotide sequences with and without the Q-codon using the Basic Local Alignment Search Tool (BLAST) revealed sufficient alterations in downstream amino acids, effectively obscuring identity in BLASTP (protein BLAST) and BLASTX (searching protein databases using a translated nucleotide query) searches. Although a single Q-codon alone was insufficient for complete concealment in BLASTN (nucleotide BLAST) searches, introducing a second Q-codon or modifying one nucleotide without altering the amino acid sequence helped achieve effective concealment (Figure 7A). Co-expressing these sequences with Q-tRNA<sub>w</sub> produced lactoferricin containing the Q-codon only in a permissive environment (Figure 7B–E). This suggests that the QCODE system can help confine genetic traits, genetic material and strains while safeguarding sequence information.

## Discussion

Here, we propose a novel biocontainment system based on a QCODE mechanism to safeguard biological resources, such as genetic traits, genetic material, engineered strains and sequence information, against unintended release. Diverging from the conventional genetic code reliant on triplet codons, we strategically inserted quadruplet codons into the coding region of genes governing heterologous metabolic pathways, essential enzymes and the proteins involved in replication initiation. In the absence of corresponding Q-tRNAs, this approach resulted in a lack of target metabolite production, cell viability and plasmid maintenance, conclusively demonstrating the ability of our system to confine genetic traits, strains and genetic material within permissive environments where Q-codons can be accurately decoded. Additionally, the system could conceal protein identity by introducing Q-codons in nucleotide sequences and inducing frameshifts in the original reading frame, confirming its capacity to protect sequence information.

Our biocontainment system is more advantageous than existing approaches, as it leverages the native translation system, eliminating the need for additional components, such as orthogonal tRNA and aminoacyl-tRNA synthetase pairs or orthogonal ribosomes, associated with decoding a new genetic code. This strategy minimizes the potential cellular burden of

incorporating multiple artificial or orthogonal systems within cells.

Furthermore, we expect that the QCODE system is generally applicable to species other than *E. coli*. Q-codons have been successfully incorporated to produce proteins in other species (42,43). We believe that the engineering efforts conducted in this study can be a useful guideline for general applications that include: (i) carefully selecting a target Q-codon based on its codon usage to minimize cross-reactions; (ii) additional genome engineering to further minimize off-target effects; and (iii) constructing a tightly regulated genetic circuit.

Our system also has limitations, including the potential occurrence of unintended frameshifts within the native genetic context when the AGG codon for arginine is followed by any codon beginning with adenine (A), resulting in mistranslation or premature termination. Such off-target decoding notably impacted cell growth in the  $\Delta argW$  strain; nonetheless, we addressed this concern by substituting AGGA with AGAA at key genomic locations, which helped to effectively reduce unintended frameshifting and restore normal cell growth. We anticipate that more comprehensive genome engineering efforts will decrease the cellular burden caused by the Q-codon. Previously, synthetic *E. coli* strains, such as syn61, were created by removing specific codons from the original genome and subsequent evolution (29). Further engineering to refine the genetic code could involve the exclusion of AGG arginine codons, potentially enhancing the QCODE efficiency. Moreover, the simultaneous utilization of Q-codons and rearranged triplet codons (27) could significantly enhance strain security and sequence encryption levels.

Another limitation of our system is the higher escape rate compared with that of state-of-the-art biocontainment systems such as synthetic polyauxotrophy (14,40,41) or refactored genetic codes (27), as previously mentioned. Cell growth repressed by the inactive QCODE system was recovered over time, indicating the limited robustness of our system. The sequence analysis showing that no colonies carried spontaneous mutations within the QCODE system may suggest that an accumulated leaky expression of the Q-tRNA in a non-permissive environment contributes to the occurrence of escapes over time. Although QCODE shows higher escape frequencies than some recent biocontainment studies due to its reliance on a single essential gene for cell killing, it introduces a novel, multilayered approach to biological containment. Unlike previous studies that primarily focused on cell growth inhibition or genetic material transfer restriction, QCODE simultaneously protects strains, genetic material, traits and sequences through a unified mechanism. The system maintains its protective function over genetic traits and materials even in cases of strain escape by blocking plasmid replication and preventing target gene expression through frameshift mechanisms. The escape frequency can be further reduced by implementing established strategies from previous studies (14,40,41,44,45). This involves incorporating multiple essential or lethal genes as killing mechanisms, introducing Q-codons across multiple genes and placing multiple Q-codons per gene within a leakiness-controlled genetic circuit. These modifications, based on validated multiple essential/lethal gene strategies from the literature, will improve the robustness of our systems. Taken together, we envisage that implementing more diverse genetic codes (46–48) and highly sophisticated designs will eventually lead to robust genetic biocontainment solutions.

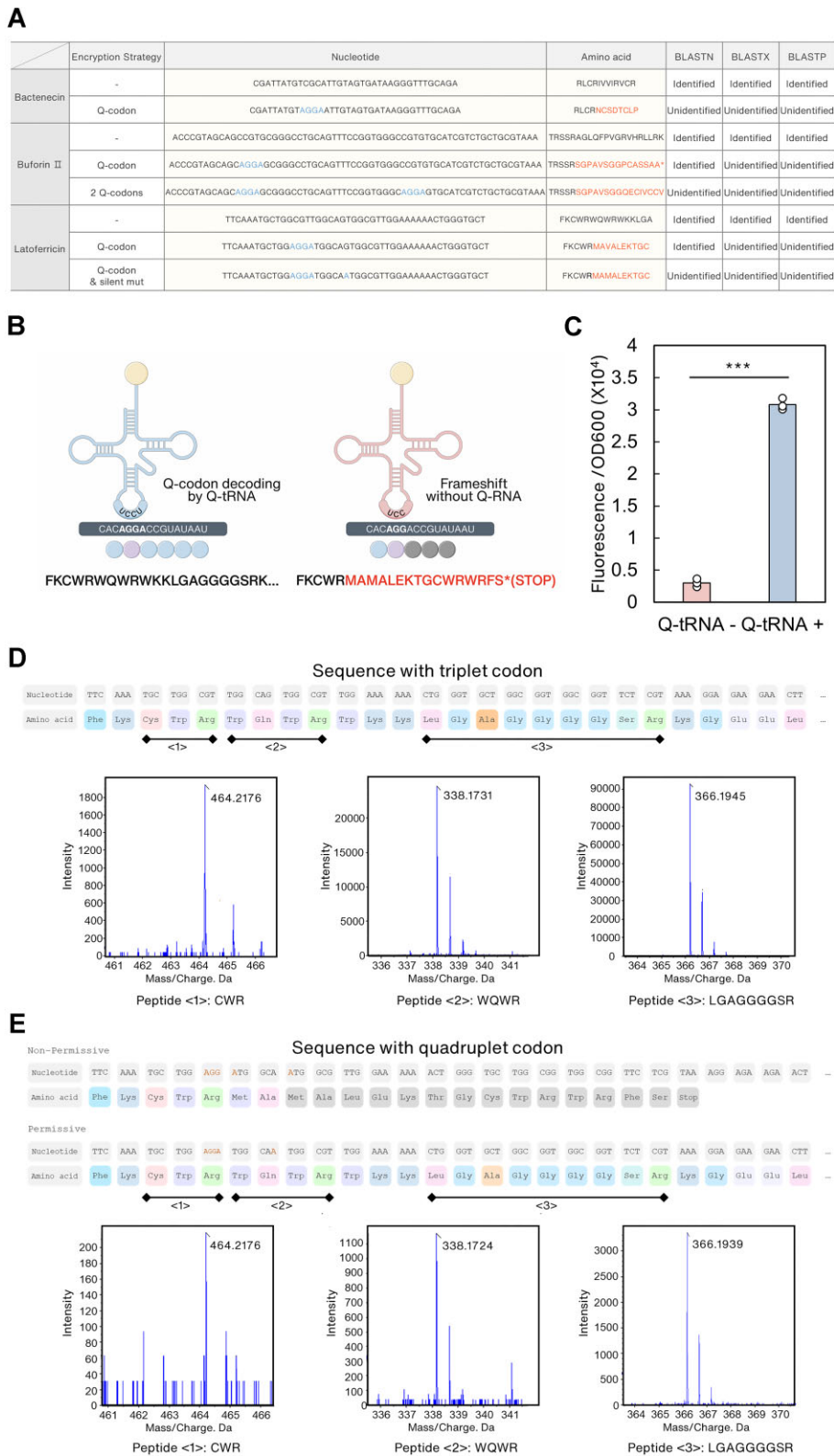


**Figure 7.** QCODE biocontainment system for sequence encryption. **(A)** BLAST analysis of three antimicrobial peptides (AMPs) testing identity concealment by including Q-codons or additional silent mutations. **(B)** Translation of lactoferricin B with and without engineered tRNA capable of reading the quadruplet codon (AGGA). **(C)** Translation of lactoferricin B-GFP fusion protein based on the QCODE system confirmed by GFP fluorescence measurement ( $n = 3$ ; error bars indicate  $\pm$  SD). Unpaired  $t$ -tests were used for comparisons.  $***P < 0.001$ . **(D, E)** Correct translation in the presence of Q-tRNA was confirmed using MALDI-TOF analysis. Peptides resulting from fragmentation around the arginine (R) encoded by the Q-codon exhibit the same mass as the positive control, which does not contain the Q-codon in the lactoferricin B sequence. The expected mass/charge values of the three fragments are 463.20017, 338.1717 and 366.1934.

## Data availability

The data underlying this article are available in the article and its online supplementary data.

## Supplementary data

Supplementary Data are available at NAR Online.

## Acknowledgements

Y.-N.C.: conceptualization, methodology, investigation, visualization, writing—original draft, writing—review & editing. D.K.: methodology, investigation, visualization, writing—original draft, writing—review & editing. S.L. and Y.R.S. investigation. J.W.L.: conceptualization, methodology, visualization, funding acquisition, project administration, supervision, writing—original draft, writing—review & editing.

## Funding

This work was supported by Samsung Research Funding & Incubation Center of Samsung Electronics (SRFC-MA1901-11). This research was also supported by the Bio & Medical Technology Development Program of the National Research Foundation (NRF) funded by the Ministry of Science & ICT (2021M3A9I4030408). This research was supported in part by the National Research Foundation (NRF) grant funded by the Korean government (MSIT) (RS-2024-00398252 and RS-2024-00466474). This work was supported partially by the Korea Medical Device Development Fund grant funded by the Korea government (the Ministry of Science and ICT, the Ministry of Trade, Industry and Energy, the Ministry of Health & Welfare, the Ministry of Food and Drug Safety) (Project Number: 1711196722, RS-2023-00254836). This research was supported in part by "Ministry of the Interior and Safety" R&D program (RS-2023-00255267). This work was also supported by the BK21 FOUR Program for Education Program for Innovative Chemical Engineering Leaders of the National Research Foundation of Korea (NRF) grant funded by the Korea government (MSIT).

## Conflict of interest statement

Patent applications have been submitted by Jeong Wook Lee, Yun-Nam Choi, Donghyeon Kim and Seongbeom Lee based on the results of this study (10-2024-0077696 (KR), 18/743720 (US), and 24182150.3 (EP)).

## References

- Mimee, M., Citorik, R.J. and Lu, T.K. (2016) Microbiome therapeutics—advances and challenges. *Adv. Drug Deliv. Rev.*, **105**, 44–54.
- Bohn, T., Aheto, D.W., Mwangala, F.S., Fischer, K., Bones, I.L., Simoloka, C., Mbeule, I., Schmidt, G. and Breckling, B. (2016) Pollen-mediated gene flow and seed exchange in small-scale Zambian maize farming, implications for biosafety assessment. *Sci. Rep.*, **6**, 34483.
- Snow, A.A. (2002) Transgenic crops why gene flow matters. *Nat. Biotechnol.*, **20**, 542.
- Stanley-Horn, D.E., Dively, G.P., Hellmich, R.L., Mattila, H.R., Sears, M.K., Rose, R., Jesse, L.C., Losey, J.E., Obrycki, J.J. and Lewis, L. (2001) Assessing the impact of Cry1Ab-expressing corn pollen on monarch butterfly larvae in field studies. *Proc. Natl Acad. Sci. USA*, **98**, 11931–11936.
- Sears, M.K., Hellmich, R.L., Stanley-Horn, D.E., Oberhauser, K.S., Pleasants, J.M., Mattila, H.R., Siegfried, B.D. and Dively, G.P. (2001) Impact of Bt corn pollen on monarch butterfly populations: a risk assessment. *Proc. Natl Acad. Sci. USA*, **98**, 11937–11942.
- Pantoja Angles, A., Valle-Perez, A.U., Hauser, C. and Mahfouz, M.M. (2022) Microbial biocontainment systems for clinical, agricultural, and industrial applications. *Front. Bioeng. Biotechnol.*, **10**, 830200.
- Arnolds, K.L., Dahlin, L.R., Ding, L., Wu, C., Yu, J., Xiong, W., Zuniga, C., Suzuki, Y., Zengler, K., Linger, J.G., et al. (2021) Biotechnology for secure biocontainment designs in an emerging bioeconomy. *Curr. Opin. Biotechnol.*, **71**, 25–31.
- Kim, D. and Lee, J.W. (2020) Genetic biocontainment systems for the safe use of engineered microorganisms. *Biotechnol. Bioproc. Eng.*, **25**, 974–984.
- Lee, J.W., Chan, C.T.Y., Slomovic, S. and Collins, J.J. (2018) Next-generation biocontainment systems for engineered organisms. *Nat. Chem. Biol.*, **14**, 530–537.
- Bahey-El-Din, M., Casey, P.G., Griffin, B.T. and Gahan, C.G. (2010) Efficacy of a *Lactococcus lactis* DeltapyrG vaccine delivery platform expressing chromosomally integrated hly from *Listeria monocytogenes*. *Bioeng. Bugs*, **1**, 66–74.
- Clark, R.L., Gordon, G.C., Bennett, N.R., Lyu, H., Root, T.W. and Pfleger, B.F. (2018) High-CO<sub>2</sub> requirement as a mechanism for the containment of genetically modified cyanobacteria. *ACS Synth. Biol.*, **7**, 384–391.
- Hirota, R., Abe, K., Katsuura, Z.I., Noguchi, R., Moribe, S., Motomura, K., Ishida, T., Alexandrov, M., Funabashi, H., Ikeda, T., et al. (2017) A novel biocontainment strategy makes bacterial growth and survival dependent on phosphite. *Sci. Rep.*, **7**, 44748.
- Steidler, L., Neiryneck, S., Huyghebaert, N., Snoeck, V., Vermeire, A., Goddeeris, B., Cox, E., Remon, J.P. and Remaut, E. (2003) Biological containment of genetically modified *Lactococcus lactis* for intestinal delivery of human interleukin 10. *Nat. Biotechnol.*, **21**, 785–789.
- Mandell, D.J., Lajoie, M.J., Mee, M.T., Takeuchi, R., Kuznetsov, G., Norville, J.E., Gregg, C.J., Stoddard, B.L. and Church, G.M. (2015) Biocontainment of genetically modified organisms by synthetic protein design. *Nature*, **518**, 55–60.
- Rovner, A.J., Haimovich, A.D., Katz, S.R., Li, Z., Grome, M.W., Gassaway, B.M., Amiram, M., Patel, J.R., Gallagher, R.R., Rinehart, J., et al. (2015) Recoded organisms engineered to depend on synthetic amino acids. *Nature*, **518**, 89–93.
- Rottinghaus, A.G., Ferreiro, A., Fishbein, S.R.S., Dantas, G. and Moon, T.S. (2022) Genetically stable CRISPR-based kill switches for engineered microbes. *Nat. Commun.*, **13**, 672.
- Stirling, F., Bitzan, L., O'Keefe, S., Redfield, E., Oliver, J.W.K., Way, J. and Silver, P.A. (2017) Rational design of evolutionarily stable microbial kill switches. *Mol. Cell*, **68**, 686–697.
- Piraner, D.I., Abedi, M.H., Moser, B.A., Lee-Gosselin, A. and Shapiro, M.G. (2017) Tunable thermal bioswitches for in vivo control of microbial therapeutics. *Nat. Chem. Biol.*, **13**, 75–80.
- Agmon, N., Tang, Z., Yang, K., Sutter, B., Ikushima, S., Cai, Y., Caravelli, K., Martin, J.A., Sun, X., Choi, W.J., et al. (2017) Low escape-rate genome safeguards with minimal molecular perturbation of *Saccharomyces cerevisiae*. *Proc. Natl Acad. Sci. USA*, **114**, E1470–E1479.
- Chan, C.T., Lee, J.W., Cameron, D.E., Bashor, C.J. and Collins, J.J. (2016) 'Deadman' and 'Passcode' microbial kill switches for bacterial containment. *Nat. Chem. Biol.*, **12**, 82–86.
- Gallagher, R.R., Patel, J.R., Interiano, A.L., Rovner, A.J. and Isaacs, F.J. (2015) Multilayered genetic safeguards limit growth of microorganisms to defined environments. *Nucleic Acids Res.*, **43**, 1945–1954.
- Cai, Y., Agmon, N., Choi, W.J., Ubide, A., Stracquadanio, G., Caravelli, K., Hao, H., Bader, J.S. and Boeke, J.D. (2015) Intrinsic biocontainment: multiplex genome safeguards combine

- transcriptional and recombinational control of essential yeast genes. *Proc. Natl Acad. Sci. USA*, **112**, 1803–1808.
23. Hall, R.J., Whelan, F.J., McInerney, J.O., Ou, Y.Q. and Domingo-Sananes, M.R. (2020) Horizontal gene transfer as a source of conflict and cooperation in prokaryotes. *Front Microbiol.*, **11**, 1569.
  24. Soucy, S.M., Huang, J. and Gogarten, J.P. (2015) Horizontal gene transfer: building the web of life. *Nat. Rev. Genet.*, **16**, 472–482.
  25. Caliando, B.J. and Voigt, C.A. (2015) Targeted DNA degradation using a CRISPR device stably carried in the host genome. *Nat. Commun.*, **6**, 6989.
  26. Nyerges, A., Vinke, S., Flynn, R., Owen, S.V., Rand, E.A., Budnik, B., Keen, E., Narasimhan, K., Marchand, J.A., Baas-Thomas, M., *et al.* (2023) A swapped genetic code prevents viral infections and gene transfer. *Nature*, **615**, 720–727.
  27. Zürcher, J.F., Robertson, W.E., Kappes, T., Petris, G., Elliott, T.S., Salmond, G.P.C. and Chin, J.W. (2022) Refactored genetic codes enable bidirectional genetic isolation. *Science*, **378**, 516–523.
  28. Robertson, W.E., Funke, L.F.H., de la Torre, D., Fredens, J., Elliott, T.S., Spinck, M., Christova, Y., Cervettini, D., Böge, F.L., Liu, K.C., *et al.* (2021) Sense codon reassignment enables viral resistance and encoded polymer synthesis. *Science*, **372**, 1057–1062.
  29. Fredens, J., Wang, K., de la Torre, D., Funke, L.F.H., Robertson, W.E., Christova, Y., Chia, T., Schmied, W.H., Dunkelmann, D.L., Beranek, V., *et al.* (2019) Total synthesis of *Escherichia coli* with a recoded genome. *Nature*, **569**, 514–518.
  30. Yu, D., Ellis, H.M., Lee, E.C., Jenkins, N.A., Copeland, N.G. and Court, D.L. (2000) An efficient recombination system for chromosome engineering in *Escherichia coli*. *Proc. Natl Acad. Sci. USA*, **97**, 5978–5983.
  31. Datsenko, K.A. and Wanner, B.L. (2000) One-step inactivation of chromosomal genes in *Escherichia coli* K-12 using PCR products. *Proc. Natl Acad. Sci. USA*, **97**, 6640–6645.
  32. Ronda, C., Pedersen, L.E., Sommer, M.O. and Nielsen, A.T. (2016) CRMAGE: CRISPR optimized MAGE recombineering. *Sci. Rep.*, **6**, 19452.
  33. Carr, P.A., Wang, H.H., Sterling, B., Isaacs, F.J., Lajoie, M.J., Xu, G., Church, G.M. and Jacobson, J.M. (2012) Enhanced multiplex genome engineering through co-operative oligonucleotide co-selection. *Nucleic Acids Res.*, **40**, e132.
  34. Isaacs, F.J., Carr, P.A., Wang, H.H., Lajoie, M.J., Sterling, B., Kraal, L., Tolonen, A.C., Gianoulis, T.A., Goodman, D.B., Reppas, N.B., *et al.* (2011) Precise manipulation of chromosomes in vivo enables genome-wide codon replacement. *Science*, **333**, 348–353.
  35. Cervettini, D., Tang, S., Fried, S.D., Willis, J.C.W., Funke, L.F.H., Colwell, L.J. and Chin, J.W. (2020) Rapid discovery and evolution of orthogonal aminoacyl-tRNA synthetase-tRNA pairs. *Nat. Biotechnol.*, **38**, 989–999.
  36. Kim, S.-W., Kim, J.-B., Ryu, J.-M., Jung, J.-K. and Kim, J.-H. (2009) High-level production of lycopene in metabolically engineered *E. coli*. *Proc. Biochem.*, **44**, 899–905.
  37. Napolitano, M.G., Landon, M., Gregg, C.J., Lajoie, M.J., Govindarajan, L., Mosberg, J.A., Kuznetsov, G., Goodman, D.B., Vargas-Rodriguez, O., Isaacs, F.J., *et al.* (2016) Emergent rules for codon choice elucidated by editing rare arginine codons in *Escherichia coli*. *Proc. Natl Acad. Sci. USA*, **113**, E5588–E5597.
  38. Konieczny, J., Doran, K.S., Helinski, D.R. and Blasina, A. (1997) Role of TrfA and DnaA proteins in origin opening during initiation of DNA replication of the broad host range plasmid RK2. *J. Biol. Chem.*, **272**, 20173–20178.
  39. Cameron, D.E. and Collins, J.J. (2014) Tunable protein degradation in bacteria. *Nat. Biotechnol.*, **32**, 1276–1281.
  40. Lopez, G. and Anderson, J.C. (2015) Synthetic auxotrophs with ligand-dependent essential genes for a BL21(DE3) biosafety strain. *ACS Synth. Biol.*, **4**, 1279–1286.
  41. Gallagher, R.R., Patel, J.R., Interiano, A.L., Rovner, A.J. and Isaacs, F.J. (2015) Multilayered genetic safeguards limit growth of microorganisms to defined environments. *Nucleic Acids Res.*, **43**, 1945–1954.
  42. O'Connor, M. (2002) Insertions in the anticodon loop of tRNA<sup>Gln</sup>(sufG) and tRNA<sup>Lys</sup> promote quadruplet decoding of CAAA. *Nucleic Acids Res.*, **30**, 1985–1990.
  43. Guo, J.T. and Niu, W. (2022) Genetic code expansion through quadruplet codon decoding. *J. Mol. Biol.*, **434**, 167346.
  44. Dunkelmann, D.L., Oehm, S.B., Beattie, A.T. and Chin, J.W. (2021) A 68-codon genetic code to incorporate four distinct non-canonical amino acids enabled by automated orthogonal mRNA design. *Nat. Chem.*, **13**, 1110–1117.
  45. Beattie, A.T., Dunkelmann, D.L. and Chin, J.W. (2023) Quintuply orthogonal pyrrolysyl-tRNA synthetase/tRNA(Pyl) pairs. *Nat. Chem.*, **15**, 948–959.
  46. DeBenedictis, E.A., Carver, G.D., Chung, C.Z., Soll, D. and Badran, A.H. (2021) Multiplex suppression of four quadruplet codons via tRNA directed evolution. *Nat. Commun.*, **12**, 5706.
  47. Hankore, E.D., Zhang, L., Chen, Y., Liu, K., Niu, W. and Guo, J. (2019) Genetic incorporation of noncanonical amino acids using two mutually orthogonal quadruplet codons. *ACS Synth. Biol.*, **8**, 1168–1174.
  48. Chatterjee, A., Lajoie, M.J., Xiao, H., Church, G.M. and Schultz, P.G. (2014) A bacterial strain with a unique quadruplet codon specifying non-native amino acids. *ChemBiochem*, **15**, 1782–1786.